2024 IEEE/RSJ International Conference on Intelligent Robots and Systems (IROS)
October 14-18, 2024. Abu Dhabi, UAE

CFD-enabled Approach for Optimizing CPG Control Network for Underwater Soft Robotic Fish

Yunfei Wang, Weiyuan Sun, Wei Tang, Xianrui Zhang, Zhenping Yu, Shunxiang Cao, Juntian Qu*

***Abstract*— Central Pattern Generators (CPG) nonlinear oscillation network is being increasingly used in the control of multi-joint collaborative robots. The motion attitude of robots can be effectively adjusted by tuning parameters of the CPG neural network. However, the mapping from CPG parameters to motion attitude is relatively complicated. To improve the motion performance, an optimization method combining computational fluid dynamics (CFD) and CPG network is proposed. In this work, we design a three-joint biomimetic soft robot fish following the body structure of trevally and an improved CPG network based on the Hopf model is incorporated into the control system. Directly optimizing the swimming performance through experiments is time consuming and complex, a mode of first adjusting parameters on the simulation platform and then refining on the robot is usually adopted. Therefore, a CFD simulation platform using hydrodynamic solutions has been established to assist in analyzing the swimming effect. Finally, the experimental results show that the swimming simulation by the CFD is highly similar to the real test, and the swimming performance after the improved CPG network optimization has been significantly increased.**

I. Introduction

In recent years, as people's exploration of the ocean has gradually deepened, more underwater detection equipment has been put into use, among which AUV and ROV have played an important role [1], [2]. Through long-term evolution, natural fish have the characteristic of efficient, flexible and fast swimming, which has attracted the attention of many researchers [3], [4]. At present, the motion performance of existing robotic fish is still inferior to that of biological fish, and the control of motion attitude has become a chief work of the development of robotic fish [3], [5]. Therefore, building a control system that can be used for bionic robotic fish to improve swimming performance through parameters optimization is necessary and achievable [6].

In the study of biological nerve signals, it is found that the central nervous system of animals is divided into the cerebral cortex, brainstem layer and spinal cord layer. Rhythmic signals can be generated through the spinal cord CPG to achieve most basic movements, such as running, breathing, swimming, etc as Fig. 1. Mathematical CPG is a lightweight neuron network that can spontaneously generate stable and rhythmic control nerve signals without input oscillation signals [7]–[9]. Transforming the connection status and synapses of neurons by higher-level control center input to change characteristics such as frequency and phase of the output signal [8], [10]. Existing CPG networks include Ijspeert's CPG model, Matsuoka's CPG model, and Hopf CPG models [9], [10]. But these CPG models are computationally time-consuming, inflexible in output signals and difficultly deployed. To obtain suitable CPG model for robot control, Shi embedded discrete Matsuoka CPG model in AVR controller [11], Xie made all the oscillators converge to the same frequency and desired phase differences based on Ijspeert's CPG model [12]. Wang combined PID to assist CPG signal to control the robotic fish [13], Shin drove bipedal robot by reinforcement learning improved CPG [14].

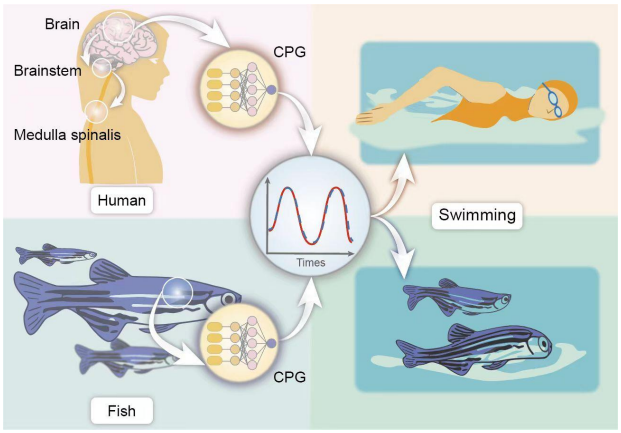

Fig. 1. CPG network for thythmic signals.

On the other hand, the hydrodynamic interaction between the fluid and the robotic fish is still complex and difficult to analyze when swimming in a static fluid environment. Therefore, it is inaccurate to rely solely on the theoretical swimming performance of dynamic analysis [15]–[17]. CFD simulation can effectively combine the kinematic model and hydrodynamics analysis to simulate the swimming performance of the robotic fish under different signals and evaluate the lift and drag generated by the fluid [18], [19]. Tuning CPG network parameters combined with CFD simulation platform can reduce experiment repetition time and improve optimization efficiency.

Motivated by the above analysis, a new swimming optimization control method for soft robotic fish is proposed.The

*J. Qu is the corresponding author. E-mail: juntian.qu@sz.tsinghua.edu.cn
This research was supported by Shenzhen "Pengcheng PeacockProgram", Beijing "Youth Talent Promotion Project" Tsinghua SIGS Crossdisciplinary Research and Innovation Fund (grant no.C2022002), Tsinghua SIGS Scientific Research Startup Fund (grant no.OD2022021C), Shenzhen Science and Technology Program (grant no.WDZC20231128114452001) and Tsinghua SIGS Overseas Research Cooperation Fund (grant no.HW2023001), Tsinghua SIGS Scientific Research Startup Fund (grant no. QD2022021C), Jianghuai Dream Fund (grant no. 2023 - ZM 01 Z006), and Shenzhen Key Laboratory of Advanced Technology for Marine Ecology (grant no.ZDSYS20230626091459009).
All authors are with SISG, Tsinghua University, Shenzhen 518055, China.

main work of this paper is as follows:

1)The Hopf model based CPG network has been upgraded. Optimizing rhythmic motion signals and generating asymmetric signals to reduce swimming resistance and improve computational efficiency. The multi-sensor feedback signals are normalized and smoothed through the set pre-processing layer which makes the robotic fish more flexibly and in line with the characteristics of biological multi-layered neural hierarchical control.

2)A 2D computational model based on the real robotic fish is imported into the CFD simulation platform. The flow field characteristics around computational fish and interaction are analyzed by CFD and hydrodynamic equations.

3)Taking the swimming performance as the optimization objective function, CPG parameters are optimized by Particle Swarm Optimization (PSO).

The effectiveness of this method is verified in real experiments. Here we improve CPG computational efficiency 5.4%,2.4%,and 4.7% respectively for different motions by simplified coupling relationship, the maximum experimental swimming speed obtained is 0.6874m/s(1.86BL/s), and the minimum experimental turning radius is 0.4947m(1.315BL).

II. Methods

A. Mechatronic Design

Based on the observation of existing fish swimming models in nature, we design a soft robotic fish like the trevally fish, which swims together with its body and pectoral fins, with streamlined body to reduce swimming resistance and improve swimming efficiency [20], [21]. The shell of robotic fish can be obtained by pouring silicone into the mold manufactured by 3D printing. Silicone (Ecoflex 00-20, smooth-on) with fabulous hydrophobicity and a Shore hardness of 20 ensures the electronic devices and a rechargeable lithium battery (DC-1210, Jianghang) are isolated from the water environment to achieve a waterproof effect, which greatly reduces the difficulty of sealing and improves the flexibility of swimming. The internal structure of the fish body includes a self-made control board, and the main microchip adopts STM32F103C8T6, which can meet the control of the serial bus servo motors (ZX-20S) and the communication function of the Bluetooth module (HC-05). The feedback data from the sensors including IR(GP2D12) and camera(HBV-1509) is returned to the microcontroller board through the serial port for closed-loop control of the robotic fish [22]–[24]. The bionic soft robotic fish has a length of 376mm and a weight of 1483.9g.

B. CPG control network

CPG is a lightweight neural network inspired by biology and widely used in the control of multiple-linked robots. By building a nonlinear oscillator, rhythmic motion signals are generated and applied to each joint. Tuning the amplitude, phase, and frequency of the joint motion signal can change the motion attitude of the robot. The CPG model has the characteristics of universality and robustness, which makes it suitable for the control of underwater robotic fish.

In the earliest studies, the Hopf CPG model consisted of only one neuron whose states are mutually inhibited, generating rhythmic signals according to the neuronal excitability and inhibition [8]. In this paper, we improve the Hopf model for better controlling of the robotic fish as Fig. 2.

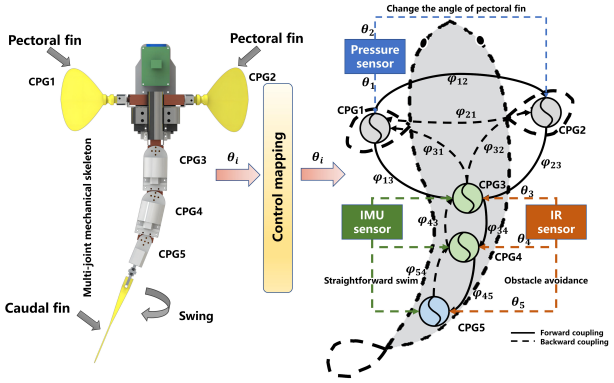

Fig. 2. CPG network topology mapping.

The single neuron expression of the typical Hopf model can be written as:

$$\begin{cases} \dot{x} = -\omega y + \mu x\left(A - x^2 - y^2\right) + \sum\left(\cos\varphi_{ij}x - \sin\varphi_{ij}y\right) \\ \dot{y} = \omega x + \mu y\left(A - x^2 - y^2\right) + \sum\left(\sin\varphi_{ij}x + \cos\varphi_{ij}y\right) \end{cases} \tag{1}$$

where, x, y represent the excitatory and inhibitory states of neurons. A, ω indicate the oscillation amplitude and frequency of neural signals respectively. μ is the convergence speed. i and j are the index number of neurons. The state of a single neuron can affect other neurons through synapses. The strength and phase relationship of this coupling described by φ_{ij} can spontaneously generate rhythmic sine waves through the Hopf oscillators. To make the Hopf CPG model more appropriate for the robotic fish, we have made the following improvements. Denoting $\Theta = A_i - x_i^2 - y_i^2$, for $i = 1,2...5$, one has the final improved CPG model as Eq.(2).

$$\begin{bmatrix} \dot{x}_i \\ \dot{y}_i \end{bmatrix} = \begin{bmatrix} \mu\Theta & -\omega_i \\ \omega_i & \mu\Theta \end{bmatrix} \begin{bmatrix} x_i \\ y_i \end{bmatrix} + \begin{bmatrix} \sum_{k=1}^{n} P(f_k) \\ 0 \end{bmatrix} + \sum_{j=1}^{5} \begin{bmatrix} \cos\varphi_{ij}x_{i-1} - \sin\varphi_{ij}y_{i-1} \\ \sin\varphi_{ij}x_{i+1} + \cos\varphi_{ij}y_{i+1} \end{bmatrix} \tag{2}$$

1)The coupling relationship between joints has been simplified. In Hopf model, the synaptic influence of neurons to all neurons is preserved, so computation is time-consuming. Only the synaptic connections of adjacent neurons are retained, which means $|i-j| = 1$ of φ_{ij} and ensures the mutual influence between joints while improving computational efficiency 5.4%,2.4%,and 4.7% respectively for different motions calculating 50 steps as shown in Fig. 5.

2)To reduce the turning radius of the robotic fish, the constant swing frequency ω is replaced. Increasing the swing frequency when the fish body swings away from the centerline of the body facing the water as ω_R, and decreasing the swing frequency as ω_D when swinging opposite to reduce the fluid resistance encountered by swimming, as shown in Eq.(3).

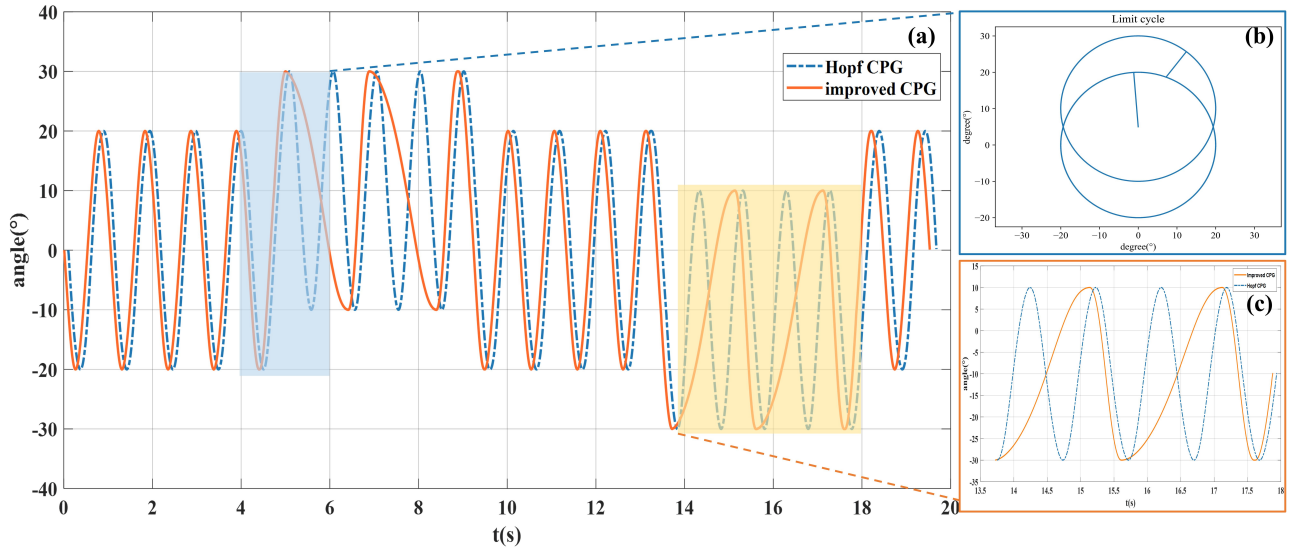

Fig. 3. (a): An example of CPG outputs for swimming. After a left turning in amplitude at time 5th second, the oscillator rapidly converges to the limit circle and remains stable as shown in (b). Asymmetric signals are generated by improved CPG to reduce turning radius as shown in (c).

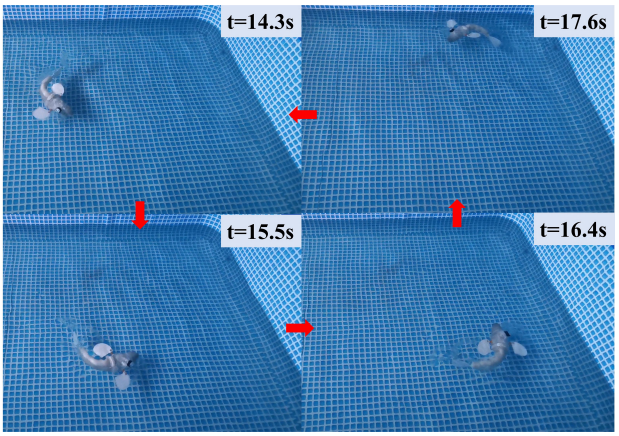

Fig. 4. Sequences figures of turning captured by high-speed camera.

$$\begin{cases} \omega_i = \frac{\omega_R}{1+e^{-\mu y_i}} + \frac{\omega_D}{1+e^{\mu y_i}} \\ \omega_R = \frac{1-\eta}{\eta}\omega_D \end{cases} \tag{3}$$

in which ω_i represent the frequency of oscillator signals generated by each neuron, ω_R, ω_D indicate the frequency of the above two opposite swing directions respectively. η is the ratio of the two frequencies of ω_R and ω_D to the oscillation period. The turning output of the CPG model also changes from a strictly symmetrical sinusoidal signal to a periodic quasi-sinusoidal signal, as shown in Fig. 3(c).

During the turning process from 14 to 18 seconds in Fig. 3(c) and Fig. 4, ω_R and ω_D replace the constant frequency to reduce the resistance. Adjusting η to change the proportion of the two frequencies, and obtain the best performance with the balance of turning time and radius.

3)For the closed-loop feedback of multi-sensors, a processing layer to receive sensory feedback signals is set, so that the sensory signals can be normalized and smoothed before entered into the CPG network, as shown in Eq.(4). The sensing signal can be regarded as the input of the high-level control center to change the signal of the low-level control center CPG. So that the fish can respond to the environment and improve its intelligence and bionicity.

$$P(f_k) = \mathrm{sgn}(\sigma_k - 0.1) * \frac{\sigma_k}{\frac{0.099}{\sigma_k} + \frac{\sigma_k}{10}} \tag{4}$$

where $\sigma_k = \frac{|f_k - f_{Std}^k|}{f_{Std}^k}$, f_k and f_{Std}^k represent the actual measured and standard value of the kth sensor respectively.

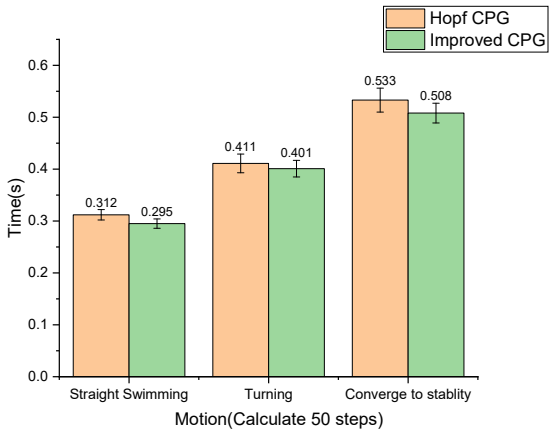

Fig. 5. Computational efficiency improved by simplified phase coupling.

III. Hydrodynamic Modeling

In this section, we introduce a set of hydrodynamic models for the robotic fish. The structure of the robotic fish is rigid-flexible coupling, so the Lagrange equation combined with CFD is chosen to analyze the swimming performance [25].

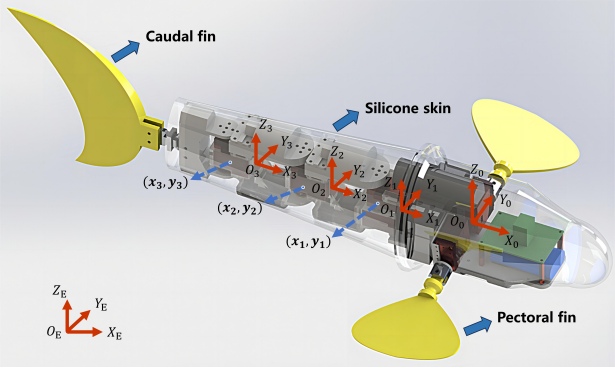

Fig. 6. Schematic illustration of coordinate frames of the robot fish.

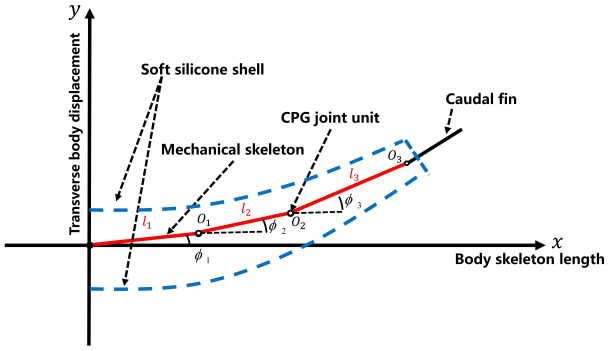

Fig. 7. Diagram of the mechanical skeleton of the robotic fish.

A. Swimming Model of Soft Robotic Fish

Signals generated by the neurons are mapped to control the corresponding servo motors has been represented in Fig. 2. The silicone of the bionic soft robotic fish isolates electronic devices from the water environment. Servo motors in the fish body are connected in series through 3D printed rigid joints to form the body skeleton. The servo motors drive the joints to swing according to the signal to generate propulsion, which is the thrust force of swimming [26], [27].

B. Dynamic Analysis Based on Lagrange Equation

The Lagrange equation is usually used to analyze the kinematics of robots. The body swing of the robotic fish can be regarded as a 3 rotation (3R) structure. To describe the force of the robotic fish clearly, we propose a coordinate system as shown in Fig. 6.

$O_E - X_E Y_E Z_E$ represents the world inertial coordinate, $O_i - X_i Y_i Z_i$ indicate the body link-fixed coordinate. The origins of $O_i - X_i Y_i Z_i$ coordinate are located at the starting point of each joint. The X_i axis points to the fish tail along the joint axis, the Y_i axis is perpendicular to the joint axis, and the Z_i axis satisfies the right spiral rule. ϕ_i are used as the relative swing angle between ith joint and $i-1$th joint. Considering that the mass distribution of the servo motors and body joints are uniform, the center of gravity of each joint is regarded as the center of the joint, expressed by coordinates (x_i, y_i).

The Lagrange equation is as follows:

$$\frac{d}{dt}\left(\frac{\partial E_k}{\partial \dot{\theta}_i}\right) - \frac{\partial E_k}{\partial \theta_i} + \frac{\partial E_p}{\partial \theta_i} = Q_i (i = 1,2,3) \tag{5}$$

where E_k and E_p indicate the kinetic energy and potential energy of the system respectively. θ_i is the generalized coordinate, and Q_i is the generalized force. The relative angular displacements ϕ_1, ϕ_2, ϕ_3 of the three joints represent generalized coordinates. Body joint moments and fluid forces are considered as generalized forces.

After proper counterweight, the gravity and buoyancy of the robot are basically the same when swimming in the water. The swimming is regarded as only in the XOY plane, so the potential energy E_p of the system can be ignored, and only the kinetic energy E_k is considered as Eq.(6).

$$E_k = \frac{1}{2} m_i v_i^2 + \frac{1}{2} J_i \omega_i^2 \quad (i = 1,2,3) \tag{6}$$

where $\omega_i = \dot{\phi}_i$, $J_i = m_i l_i^2$. Considering that the quality of the joints is evenly distributed, $v_{xi} = \dot{x}_i, v_{yi} = \dot{y}_i$ are chosen to represent the instantaneous velocities of the intermediate points of each joint. ϕ_i are the swimming signals generated by the CPG network. J_i indicate the moment of inertia of each joint, and the length of the joint ith is l_i shown in Fig. 7. To show the interaction force between the robotic fish body and the fluid clearly, denoting $L_a = l_2 \sin\phi_3 + l_1 \sin(\phi_2 + \phi_3)$, $L_b = l_2 \cos\phi_3 + l_1 \cos(\phi_2 + \phi_3)$, $L_c = l_2 \sin\phi_3$, $L_d = l_2 \cos\phi_3$. According to the principle of virtual work, the Jacobian matrix of the system force is the transpose of its motion Jacobian matrix. Based on Fig. 7, Jacobian of the force relative to the world coordinate system is expressed as Eq.(7), which converts force to the same coordinate system.

$$J^T = \begin{bmatrix} L_a & L_b & 0 & 0 & 0 & 1 \\ L_c & L_d & 0 & 0 & 0 & 1 \\ 0 & 0 & 0 & 0 & 0 & 1 \end{bmatrix} \tag{7}$$

The reaction force of the fluid field on the fish body can be expressed as the following matrix.

$$D = \begin{bmatrix} F_x & F_y & 0 & 0 & 0 & M_z \end{bmatrix}^T \tag{8}$$

where F_x and F_y are the lateral and longitudinal forces of the vortex on the fish body, which are obtained by combining the lift and drag generated by the fluid, and M_z represents the torque in the z-axis direction.

According to Eq.(7) and Eq.(8), the mapping relationship between the external force on the fish body and the driving force generated by the joints of the fish body is as follows:

$$F_T = J^T D = \begin{bmatrix} F_x L_a + F_y L_b + M_z \\ F_x L_c + F_y L_d + M_z \\ M_z \end{bmatrix} \tag{9}$$

The Lagrange equation is further expressed as Eq.(10).

$$\begin{bmatrix} \frac{d}{dt}\left(\frac{\partial E_k}{\partial \dot{\phi}_1}\right) - \frac{\partial E_k}{\partial \phi_1} \\ \frac{d}{dt}\left(\frac{\partial E_k}{\partial \dot{\phi}_2}\right) - \frac{\partial E_k}{\partial \phi_2} \\ \frac{d}{dt}\left(\frac{\partial E_k}{\partial \dot{\phi}_3}\right) - \frac{\partial E_k}{\partial \phi_3} \end{bmatrix} - \begin{bmatrix} F_x L_a + F_y L_b + M_z \\ F_x L_c + F_y L_d + M_z \\ M_z \end{bmatrix} = \begin{bmatrix} T_1 \\ T_2 \\ T_3 \end{bmatrix} \tag{10}$$

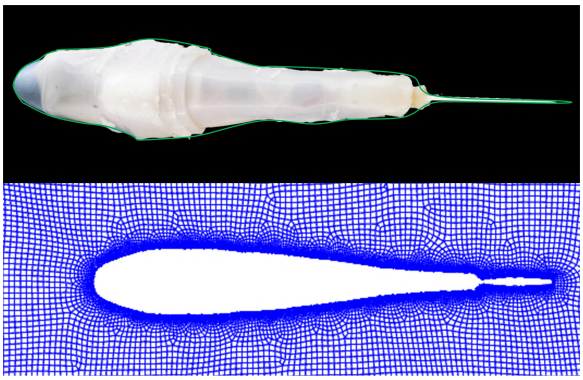

Fig. 8. The real robotic fish and mesh around computational fish.

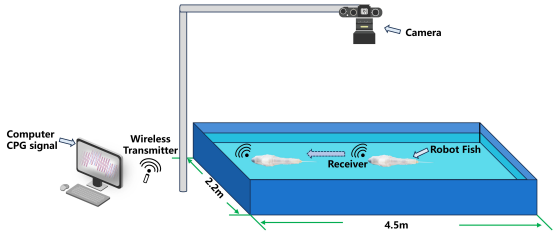

Fig. 9. Experimental platform for testing swimming performance.

where T_1, T_2, T_3 are the rotational torques of joints respectively. The generalized forces of the fluid determined by the Lagrange equation are analyzed in the following subsection.

C. Hydrodynamic analysis

In the swimming experiment platform, we suppose the fluid around the robotic fish to be non-rotating, non-viscous, and incompressible for the convenience of calculation. Based on the uniform distribution of joint mass, the fluid force can be regarded as acting on the centroid (x_i, y_i) of each joint. Therefore, the additional mass force and viscous resistance on the joint can be written as:

$$F_{\xi i} = \begin{bmatrix} F_{\xi xi} \\ F_{\xi yi} \end{bmatrix} = m_{\xi i} \begin{bmatrix} \dot{v}_{xi} \\ \dot{v}_{yi} \end{bmatrix} \tag{11}$$

where $m_{\xi i}$ represent the additional mass coefficient, which is a dimensionless constant related to the shape of the joint and the direction of motion. $F_{\xi xi}$, $F_{\xi yi}$ respectively represent the additional mass force generated by the x-axis and y-axis movement, and the force of the fluid is related to the acceleration of the joint.

$$F_{\sigma i} = \begin{bmatrix} F_{\sigma xi} \\ F_{\sigma yi} \end{bmatrix} = \begin{bmatrix} -\frac{1}{2}\Delta_{xi}\rho S_{xi} v_{xi}^2 \\ -\frac{1}{2}\Delta_{yi}\rho S_{yi} v_{yi}^2 \end{bmatrix} \tag{12}$$

where S_{xi}, S_{yi} and Δ_{xi}, Δ_{yi} respectively represent the cross-sectional area of the joint YOZ, XOZ plane and the friction force of the plane fluid, ρ indicates the density of the environment fluid. It is worth noting that the forward direction of the robotic fish in this paper is the negative direction of the x-axis. To simplify the calculation, only the force on the first joint along the x-axis can be considered. The lift force, drag force and swinging moment on the caudal fin are the resultant force that propels the fish to swim forward, we analyze the force of the fluid acting on the fish tail.

$$\begin{cases} C_x = \int_S C_p n_x ds \\ C_y = -\int_S C_p n_y ds \\ C_{MZ} = \iint_S C_p (x n_y - y n_x) ds \end{cases} \tag{13}$$

where the bow thrust coefficient C_x of the tail fin, the lateral force coefficient C_y, and the moment coefficient of C_{MZ} around the z-axis. n_x and n_y represent the axial component of the unit normal vector on the surface of the caudal fin,S is the area of caudal fin, and C_p is the pressure coefficient on the surface of the caudal fin, which is defined as follows Eq.(14).

$$\begin{cases} C_x = \dfrac{F_x}{1/2\rho V_{cx}^2 C_0 B \cos\alpha} \\ C_y = \dfrac{F_y}{1/2\rho V_{cy}^2 C_0 B |\sin\alpha|} \\ C_{mz} = \dfrac{M_z}{1/2\rho V_{\omega}^2 C_0^2 B} \end{cases} \tag{14}$$

where ρ represents the density of the fluid, B is the span of the caudal fin, C_0 indicates the characteristic chord length of the caudal fin, and α is the angle between the fish tail and the incoming flow. V_{cx}, V_{cy}, V_{ω} respectively represent the speed of the fish tail in the world coordinate system. Substituting Eq.(14) into Eq.(10), the final form of the system Lagrange equation can be obtained Eq.(15).

According to the above dynamic analysis, we can get the thrust forces as Eq.(15) along the x-axis and y-axis.

$$F_{Thrust} = \begin{bmatrix} F_{Tx} \\ F_{Ty} \end{bmatrix} = \begin{bmatrix} F_x - \sum F_{\xi xi} - F_{\sigma xi} \\ F_y - \sum F_{\xi yi} - F_{\sigma yi} \end{bmatrix} \tag{15}$$

Newton's second law is used to analyze the relationship between the propulsion force and the speed of the robotic fish, we can obtain the theoretical swimming speed as Eq.(16).

$$\int_0^T V_c(t)^2 dt = k \int_0^T F_{Thrust} dt \tag{16}$$

where $k = -\frac{2}{\rho C_x S_{x1}}$ represents the drag coefficient.

IV. Results

To improve the accuracy and authenticity of the simulation with the complexity of the actual environment, CFD combined with real experiments is used to verify the effectiveness of the improved CPG network. Experiment environment is shown as Fig. 9 and PSO is applied for tune parameters for better swimming performance.

A. CFD simulation

In this paper, the robotic fish is only focused on the XOY plane. Therefore, 3D simulation is computationally slow and unnecessary, and 2D space mesh has been built as Fig. 8. The boundary of the space is set as a circle with a diameter of 25 body lengths. The model of fish is imported from SolidWorks of the physical robotic fish during simulation, and the silicone skin is idealized. The movement adopts the joint signals generated by the CPG network, which is consistent with the real robotic fish [28], [29]. In the CFD

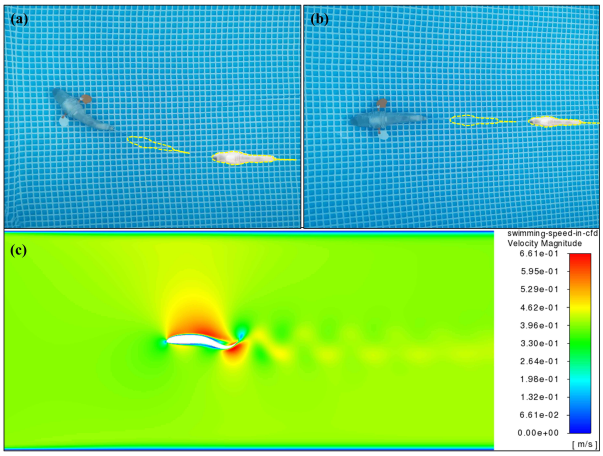

Fig. 10. Simulation and experimental results.The initial position and swimming trajectory are represented respectively by the fish image and dotted lines. (a) Turning right to obtain the radius by signals generated by improved CPG network. (b) Swimming straight to test the speed of the robotic fish. (c) Simulation in CFD is shown.

environment built in Ansys, the robotic fish is simulated to swim straight and turn around. The swimming performance under different CPG parameters is tested in combination with real experiments and shown as Fig. 10.

Algorithm 1 Pseudocode of Swimming Performance Optimization

Input: $\mathbf{R_0}$: initial parameters of CPG network;
$\mathbf{R_{new}}$: current parameters of CPG network;
$iter_{max}$: maximum iteration;
V_{new}: current swimming speed;
r_{new}: current turning radius;
Output: optimal state : V_{max} and r_{min}

repeat
  Simulate $\mathbf{R_{new}}$ in CFD;
  Calculate $\int_0^T V_c(t)^2 dt = k \int_0^T F_{Thrust} dt$;
  if $V_{max}<V_{new}$ or $r_{min}>r_{new}$ **then**
    Update V_{max} and r_{min};
  end if
until $iter=iter_{max}$
return V_{max} and r_{min}.

B. Swimming performance optimization by PSO

PSO is a random search algorithm developed to simulate the foraging behavior of a flock of birds, and is widely used in parameter optimization. Taking the straight swimming speed and the minimum turning radius as the objective function, by tuning CPG parameters and simulating swimming performance in CFD up to the maximum number of iterations, the best swimming performance parameters are selected for real experimental comparison.

Each time a set of parameters is input, the simulation platform iterates to the max number of times and initializes before the next input. The results obtained by optimizing swimming speed and turning radius are shown in Fig. 11, and the comparsion with other robotic fish is in Table.I.

The error between simulation and experimental results is guaranteed to be within 10%, proving the effectiveness of the method. After 50 iterations, the maximum experimental swimming speed is 0.6874m/s(1.86BL/s), and the minimum experimental turning radius is 0.4947m(1.315BL).

TABLE I
COMPARSION WITH CLASSIC BIONIC PLARFORMS

Platform	Body Length(m)	Speed(m/s)	Speed(BL/s)
Robotic pike [33]	0.46	0.61	0.75
CasiTuna [34]	0.52	0.80	1.52
T-fish [30]	0.45	0.47	1.04
Wire-driven fish [32]	0.31	0.67	2.15
ours	0.37	0.69	1.86

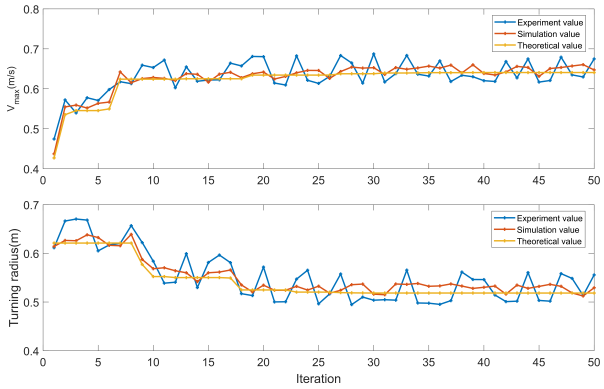

Fig. 11. Comparison of 50 iteration optimization results of swimming speed and turning radius.

V. CONCLUSIONS

In this work, we propose computational fluid dynamics as a method for optimizing CPG network for underwater soft robotic fish swimming performance. This method based on improved CPG network and CFD whose core relies on using CFD simulation combined with PSO to find the best network parameters and improve the optimization speed. Simulation and experimental results show that both the swimming speed and the minimum swimming radius are improved.

As future work, we plan to combine the 3D CFD model to simulate the complex movements of the robotic fish to further improve the simulation accuracy. Moreover, our goal is to establish a data-driven experimental platform for real-time control of robotic fish.

REFERENCES

[1] A. Mazzeo, J. Aguzzi, M. Calisti, S. Canese, F. Vecchi, S. Stefanni, and M. Controzzi, "Marine Robotics for Deep-Sea Specimen Collection: A Systematic Review of Underwater Grippers," *Sensors*, vol. 22, no. 2, 2022.

[2] J. Qu, Y. Xu, Z. Li, Z. Yu, Y. Wang, et al., "Recent Advances on Underwater Soft Robots," *Advanced & Intelligent Systems*, vol. 6, no. 2, pp. 20–29, 2023.

[3] R. Aditi and T. Atul, "Fish-inspired robots: design, sensing, actuation, and autonomy—a review of research," *Bioinspiration & biomimetics*, vol. 11, no. 3, 2016.

[4] W. Tang, Y. Wang, and Z. Yu, et al. "Bionic Robotic Fish Mechanical Structure Optimization Design and Performance Analysis Based on Fluent," *2023 IEEE 19th International Conference on Automation Science and Engineering (CASE)*, pp. 1–6, 2023.

[5] M. Anton, Z. Chen, M. Kruusmaa, and X. B. Tan, "Analytical and computational modeling of robotic fish propelled by soft actuation material-based active joints," in *2009 IEEE/RSJ International Conference on Intelligent Robots and Systems*, pp. 2126–2131, 2009.

[6] J. M. Blank, C. J. Farwell, J. M. Morrissette, R. J. Schallert, and B. A. Block, "Influence of swimming speed on metabolic rates of juvenile Pacific bluefin tuna and yellowfin tuna," *Physiological and Biochemical Zoology*, vol. 80, no. 2, pp. 167–177, 2007.

[7] Gen Endo, Jun Morimoto, Takamitsu Matsubara, Jun Nakanishi, and Gordon Cheng, "Learning CPG-based biped locomotion with a policy gradient method: Application to a humanoid robot," *The International Journal of Robotics Research*, vol. 27, no. 2, pp. 213–228, 2008.

[8] M. Wang, J. Yu, M. Tan, and G. Zhang, "A CPG-based sensory feedback control method for robotic fish locomotion," in *Proceedings of the 30th Chinese Control Conference*, pp. 4115-4120, 2011.

[9] A. J. Ijspeert, "Central pattern generators for locomotion control in animals and robots: A review," *Neural Networks*, vol. 21, no. 4, pp. 642-653, 2008.

[10] K. Matsuoka, "Sustained oscillations generated by mutually inhibiting neurons with adaptation," *Biological Cybernetics*, vol. 52, no. 6, pp. 367-376, 1985.

[11] Li. L, Wang. C, and Xie. G, "A general CPG network and its implementation on the microcontroller," *Neurocomputing*, vol. 167, pp. 299-305, 2015.

[12] Y. Wang, W. Sun, W. Tang, and Z. Yu, "A Swimming Performance Optimization Method for Achieving Low Cost of Transport of Soft Robotic Fish," in *ISOPE International Ocean and Polar Engineering Conference (ISOPE)*, pp. ISOPE-I-24-269, 2024.

[13] J. Qu, Z. Yu, W. Tang, et al. "Advanced Technologies and Applications of Robotic Soft Grippers," *Advanced Materials Technologies*, vol. 9, no. 11, 2024.

[14] Zhao. W, Yu. J, and Fang. Y, "Development of multi-mode biomimetic robotic fish based on central pattern generator," *2006 IEEE/RSJ International Conference on Intelligent Robots and Systems*, pp. 3891-3896, 2006.

[15] D. Costa, M. Franciolini, G. Palmieri, A. Crivellini, and D. Scaradozzi, "amics analysis and design of an ostraciiform swimming robot," in *2017 IEEE International Conference on Robotics and Biomimetics* , pp. 135-140, 2017.

[16] Y. H. Zhang, J. H. He, J. Yang, S. W. Zhang, and K. H. Low, "A computational fluid dynamics (CFD) analysis of an undulatory mechanical fin driven by shape memory alloy," *International Journal of Automation and Computing*, vol. 3, no. 4, pp. 374–381, 2006.

[17] H. Chung and S. Cao and M. Philen, "CFD-CSD coupled analysis of underwater propulsion using a biomimetic fin-and-joint system," *Computers & Fluids*, vol. 172, pp. 54-66, 2018.

[18] H. Zhou, T. J. Hu, H. B. Xie, D. B. Zhang, and L. C. Shen, "Computational hydrodynamics and statistical modeling on biologically inspired undulating robotic fins: a two-dimensional study," *Journal of Bionic Engineering*, vol. 7, no. 1, pp. 66–76, 2010.

[19] Y. Takada, T. Ochiai, N. Fukuzaki, T. Tajiri, and T. Wakisaka, "Analysis of flow around robotic fish by three-dimensional fluid-structure interaction simulation and evaluation of propulsive performance," *Journal of Aero Aqua Bio-mechanisms*, vol. 3, no. 1, pp. 57–64, 2013.

[20] L. Li, C. Wang, and G. M. Xie, "A general CPG network and its implementation on the microcontroller," *Neurocomputing*, vol. 167, no. 2015, pp. 299–305, 2015.

[21] L. Li, A. Q. Liu, W. Wang, S. Ravi, R. B. Fu, J. Z. Yu, and G. M. Xie, "Bottom-level motion control for robotic fish to swim in groups: modeling and experiments," *Bioinspiration & biomimetics*, vol. 14, no. 4, p. 046001, 2019.

[22] Q. Ren, J. Xu, and X. Li, "A data-driven motion control approach for a robotic fish," *Journal of Bionic Engineering*, vol. 12, no. 3, pp. 382–394, 2015.

[23] A. Ming, K. Hashimoto, W. Zhao, and M. Shimojo, "Fundamental analysis for design and control of soft fish robots using piezoelectric fiber composite," in *2013 IEEE International Conference on Mechatronics and Automation*, pp. 219-224, 2013.

[24] N. Kamamichi, M. Yamakita, K. Asaka, and L. Zhi-Wei, "A snake-like swimming robot using IPMC actuator/sensor," in *2006 IEEE International Conference on Robotics and Automation*, pp. 1812-1817, 2006.

[25] W. Zhao, A. Ming, and M. Shimojo, "Dynamic analysis and fluid-structural coupling method," in *2014 IEEE International Conference on Robotics and Automation* , pp. 1474-1479, 2014.

[26] B. Lu, C. Zhou, J. Wang, Y. Fu, L. Cheng, and M. Tan, "Development and stiffness optimization for a flexible-tail robotic fish," *IEEE Robotics and Automation Letters*, vol. 7, no. 2, pp. 834–841, 2022.

[27] S. Zhang, X. Qian, Z. Liu, Q. Li, and G. Li, "PDE modeling and tracking control for the flexible tail of an autonomous robotic fish," *IEEE Transactions on Systems, Man, and Cybernetics*, vol. 52, no. 12, pp. 7618–7627, 2022.

[28] M. Nakabayshi, Y. Yamaguchi, and W. Yamazaki, "Numerical optimization of thrust efficiency of propulsion in fluid using a fin with variable stiffness," *Journal of Aero Aqua Bio-mechanisms*, vol. 5, no. 1, pp. 1–9, 2016.

[29] Y. Wang, W. Sun, W. Tang, Z. Yu, et al. "Swimming Optimization Method of Soft Bio-inspired Robotic Fish Based on Improved CPG Model," in *2023 IEEE International Conference on Automation Science and Engineering (CASE)*, pp. 1–6, 2023.

[30] Qiu. C, Wu. Z, Wang. J, Tan. M, and Yu. J, "Locomotion optimization of a tendon-driven robotic fish with variable passive tail fin," *IEEE Transactions on Industrial Electronics*, vol. 70, no. 5, pp. 4983-4992, 2022.

[31] Tong. R, Wu. Z, and Chen. D, "Design and optimization of an untethered high-performance robotic Tuna," *IEEE/ASME Transactions on Mechatronics*, vol. 27, no.5, pp. 4132-4142, 2022.

[32] Zhong. Y, Li. Z, and Du. R, "A novel robot fish with wire-driven active body and compliant tail," *IEEE/ASME Transactions on Mechatronics*, vol. 22, no. 4, pp. 1633-1643, 2017.

[33] Z. Wu, J. Yu, Z. Su, M. Tan, and Z. Li, "Towards an Esox lucius inspired multimodal robotic fish," *Science China. Information Sciences*, vol. 58, no. 5, pp. 1–13, 2015

[34] S. Du, Z. Wu, J. Wang, S. Qi, and J. Yu, "Design and control of a two-motor actuated tuna-inspired robot system," *IEEE Transactions on Systems, Man, and Cybernetics Systems*, vol. 51, no. 8, pp. 4670–4680, 2021.